Ocean Sci. J. (2020) 55(1):33–48
http://dx.doi.org/10.1007/s12601-020-0012-z

Available online at http://link.springer.com

SpringerLink

Article

Ocean Science Journal

pISSN 1738-5261
eISSN 2005-7172

Morphological Variation of the Sea Silverside *Odontesthes regia* in Regions with Dissimilar Upwelling Intensity along the Humboldt Current System

Diego Deville[1], Gustavo Sanchez[1], Sergio Barahona[2], Carmen Yamashiro[3], Daniel Oré-Chávez[2], Roger Quiroz Bazán[2], and Tetsuya Umino[1]*

[1]*Graduate School of Integrated Sciences for Life, Hiroshima University, Higashihiroshima 739-8528, Japan*
[2]*Facultad de Ciencias Biológicas, Laboratorio de Ecología Molecular y Biodiversidad Acuática, Universidad Nacional Mayor de San Marcos, Lima 15081, Peru*
[3]*Dirección General de Investigaciones de Recursos Demersales y Litorales, Instituto del Mar del Perú, Callao 07021, Peru*

Received 3 October 2019; Revised 4 December 2019; Accepted 8 January 2020

Abstract – We evaluated the influence of areas with dissimilar upwelling intensity along the Humboldt Current System on the morphological variation of the economically important sea silverside *Odontesthes regia* by using geometric morphometric (GM) and meristic data of populations sampled off Northern Peru, Central Peru, Southern Peru-Northern Chile, and Central-Southern Chile (CSCH). Multivariate analyses of variance, a UPGMA tree, and discriminant analyses of meristic counts separated CSCH individuals, which had slightly higher numbers of gill rakers and radius of the anal fin. Permutation tests and canonical variate analyses of GM data distinguished all populations and highlighted deformations in the head and fins. Variations in GM and meristic analyses were significantly correlated with values of the sea surface temperature and surface chlorophyll-a concentrations. Morphological differences among populations might be associated with the spatial coastal upwelling dynamic of the Humboldt Current System, which highlights the role that this system plays in relation to the phenotypic variation of fish.

Keywords – coastal species, geometric morphometrics, meristics, phenotypic variation, Southeastern Pacific Ocean

1. Introduction

The Humboldt Current System (HCS) is one of the most productive eastern boundary upwelling ecosystems in the world (Chavez et al. 2008). It spans more than 40° of latitude, ranging from the north of Peru (~4°S) where cold upwelled waters encounter warm tropical waters, to the south of Chile (~45°S) but exerts less influence in waters of the Inner Sea of Chiloe (ISCh), a continuous series of estuarine deep basins (Zapata-Hernández et al. 2016). Since the upwelling intensity along the HCS is not uniform, Montecino and Lange (2009) divided it into three subsystems: (1) a permanent productive, from northern to central Peru (~13°S) with sea surface temperatures (SST) around 19°C and salinity levels above 34.9‰ (Silva et al. 2009); (2) a lower productive but with larger upwelling from southern Peru to northern Chile (~15–26°S) with SST between 14°C to 16°C and salinity around 34.9‰ (Silva et al. 2009); and (3) a seasonal productive from central (~ 34°S) to southern Chile (Fig. 1) with SST from 12°C to 13.5°C, salinity from 33.5‰ to 33.9‰ (Silva et al. 2009), and a maximum upwelling and productivity in austral summer (January–March) (Montecino and Lange 2009).

The productivity of the upwelling in the HCS is associated with high concentrations of phytoplankton (i.e., primary production), which plays an essential role in higher trophic categories and the growth development of species. Primary production can be estimated as a function of the photosynthetic response on chlorophyll-a concentration (Sathyendranath and Platt 2001). The high productivity of the HCS is a consequence of the coastal upwelling dynamics of this ecosystem (Montecino and Lange 2009). There are significant differences in the annual surface chlorophyll-a (Chl-a) concentrations between the subsystems of the HCS despite the seasonal mismatch between upwelling coastal winds and Chl-a concentration off Peru (Echevin et al. 2008). Differences in upwelling intensity and temperature play an important role in the abundance of fish, food, nutrients (Montecino and Lange 2009), and the

*Corresponding author. E-mail: umino@hiroshima-u.ac.jp

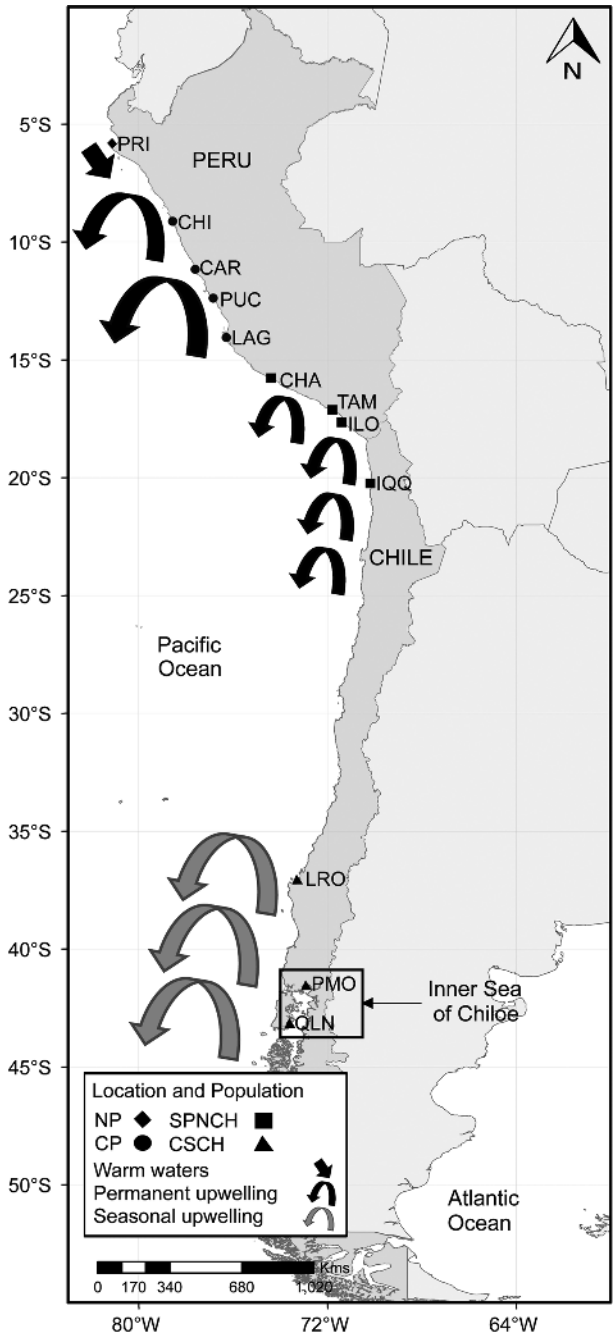

Fig. 1. Upwelling subsystems of the Humboldt Current (adapted from Montecino and Lange 2009), the Inner Sea of Chiloe and locations where sea silverside (*Odontesthes regia*) were sampled in 2015 and 2018

phenotype of species (Lindsey 1988).

Morphometric and meristic analyses are useful to assess the variation in marine populations (Murta et al. 2008) as a response to the environmental conditions on a short timescale (Heino 2014). Morphometric characters are continuous descriptors of the body shape. Deviation of these characters describe differences in growth rates and maturation conditions, which are strongly related to phenotypic characteristics of populations (Booke 1981). On the other hand, meristic characters such as fin rays, scales, and gill rakers are discrete components of fish that reveal whether early development occurred in independent areas (Swain et al. 2005). The assessment of morphological variation in populations is also useful for stock management of species (Murta et al. 2008) since populations with similar morphological variation share similar life history characters (Hilborn and Waters 1992) and could be similarly managed.

To date, studies assessing the morphological variation of marine invertebrates along the HCS suggest a phenotypic variation influenced by the environmental conditions of the HCS. For example, Haye et al. (2010) reported that the vertical boundary of the oxygen minimum zone is an important condition for the development of a pelagic (up to 25°S) and a benthonic (south to 25°S) form in the squat lobster *Pleuroncodes monodon*. Vega et al. (2002) explained that morphological differences of the coastal squid *Doryteuthis gahi* along the HCS might be related to the temperature and salinity levels. However, in contrast to marine invertebrates, marine fish should respond differently to environmental variations due to their contrasting life strategies and corporal structures.

Odontesthes is a genus with nineteen recently radiated species (García et al. 2014) restricted to South America (Dyer 2006). A high phenotypic variation (González-Castro et al. 2016) and local adaptation to contrasting environmental conditions have been reported in *Odontesthes* species (Beheregaray and Sunnucks 2001; Beheregaray and Levy 2000). Among them, the sea silverside *Odontesthes regia* (Humboldt, 1821) is the only species that inhabits shallow marine and estuarine waters along the HCS, from Punta Aguja (5°S, Northern Peru) to Los Chonos Islands (46°S, southern Chile) (Dyer and Gosztonyi 1999). The sea silverside supports important fishery activities with annual landings of around 5000 t in Peru (http://www.ogeiee.produce.gob.pe/) and 1500 t in Chile (http://www.sernapesca.cl/informes/estadisticas). Studies addressing the morphological variation of *O. regia* in the HCS are limited to the use of meristic counts that suggest a southward latitudinal increase in the number of anal-fin rays, gill rakers, and caudal vertebrae along this system (Dyer and Gosztonyi 1999). The wide-range distribution of the sea silverside and the morphological adaptation observed in closely related species, make *O. regia* a suitable species to

assess the influence of the different upwelling intensities of the HCS on the morphological variation of marine fish. Therefore, this study aimed to assess the influence of the different upwelling areas along the HCS on the morphological variation of *O. regia* through the analyses of meristic and geometric morphometric data.

2. Material and Methods

Sampling and data collection

A total of 842 fresh individuals were collected during the summer of 2015 and 2018, along 12 different locations (Fig. 1; Table 1). To avoid the collection of closely related species in some locations, we used the taxonomic traits proposed by Dyer (2006) to identify individuals at the species level. Digital photography from the left side of each fish was taken with a Nikon D3200 camera (Len 18–50 mm, 24 MP) only from individuals collected in 2018.

In all the individuals from both years, five meristic characters previously used to assess variation in the subgenus *Austromenidia* (*O. regia*, *O. gracilis* and *O. smitti*) (Dyer and Gosztonyi 1999) were counted by the same person using a stereoscopic microscope: (1) radius of the first dorsal fin (RD1), (2) the second dorsal fin (RD2), (3) the anal fin (RA); and gill rakers of (4) the upper branch (GRU), and (5) the lower branch (GRL) of the first gill arch from the left side. The independence of these characters with respect to size was evaluated by the non-significance ($P > 0.05$) of Pearson's correlation coefficients in all the data, populations and locations; and by ANOVAs using each character as a factor.

In geometric morphometric analysis, we digitized 18 landmarks (L1–L18) (Fig. 2) using TpsDig v2.31 (Rohlf 2017). We used the unbending routine in TpsUtil v1.78 (Rohlf 2018) with L1, L7, L16, 17 and L18 to correct body position, and then removed the last two for posterior analyses. Landmark configurations were aligned, rotated, translated, and scaled by a Generalized Procrustes Analysis (GPA) (Rohlf and Slice 1990). The centroid size was calculated as a measure of size for all the individuals. Since Procrustes coordinates were significantly correlated ($P < 0.001$) with log-transformed centroid size, we used residuals from this regression in further analyses. Then, a mean landmark configuration from all the samples was calculated, herein the consensus shape.

Statistical comparisons

Firstly, multivariate analyses of variance (MANOVA) were used to evaluate significant differences among locations and populations. Then, the stepwise discriminant analysis (SWDA) available in SPSS v.24.0 was used to assess the degree of similarity and the relative importance of each meristic character in the differentiation of locations and populations. Cross-validated classification values were used to check the amount of similarity among locations and populations. The relationship among locations was estimated in a UPGMA tree of Mahalanobis distances.

We performed permutation tests of 10000 replicates to assess significant differences of mean Procrustes distances

Table 1. Summary information of the sea silverside (*Odontesthes regia*) sampled off Northern Peru (NP), Central Peru (CP), Southern Peru and Northern Chile (SPNCH), and Central and Southern Chile (CSCH) in 2015 and 2018. COD: sample code, n: number of individuals GM: geometric morphometric data, Me: meristic counts. TL: total length, Max: maximum, Min: minimum

Population	Location	COD	n (GM/Me)	Sampling date	TL (mm)		Meristic counts [Min–Max (Mean)]				
					Min–Max	Mean	RD1	RD2	RA	GRU	GRL
NP	Puerto Rico	PRI	0/101	03/15	168.5–247.8	207.7	6–9 (7)	9–12 (11)	14–18 (17)	8–11 (9)	22–28 (25)
CP	Chimbote	CHI	121/121	02/18	106.3–202.5	161.1	5–8 (7)	10–12 (11)	15–19 (17)	7–10 (9)	21–28 (25)
	Carquin	CAR	77/81	02/18	137.2–177.7	160.9	5–8 (7)	10–12 (11)	15–19 (17)	7–10 (9)	21–28 (25)
	Pucusana	PUC	77/71	01/18	113.9–175.9	149.0	4–8 (7)	10–12 (11)	16–19 (17)	7–9 (8)	21–28 (25)
	Lagunilla	LAG	81/81	01/18	112.4–180.4	148.4	5–8 (7)	9–14 (11)	15–19 (17)	7–10 (9)	21–27 (25)
SPNCH	Chala	CHA	81/82	02/18	135.1–190.5	165.8	4–8 (6)	10–12 (11)	15–19 (17)	7–10 (9)	23–28 (25)
	Tambo	TAM	0/46	03/15	118.7–170.1	143.5	5–8 (7)	10–12 (11)	15–19 (17)	8–9 (9)	21–28 (25)
	Ilo	ILO	0/60	03/15	127.8–155.4	140.8	5–8 (7)	10–12 (11)	15–19 (17)	6–9 (8)	21–29 (25)
	Iquique	IQQ	50/50	03/18	144.8–189.5	159.8	5–8 (7)	10–12 (11)	16–19 (17)	7–10 (9)	21–28 (25)
CSCH	Lo Rojas	LRO	61/40	03/18	209.4–271.7	234.3	5–9 (7)	9–12 (11)	16–20 (18)	8–10 (9)	23–28 (26)
	Puerto Montt	PMO	39/39	03/18	217.6–267.9	240.5	5–8 (7)	10–13 (11)	16–20 (18)	8–12 (9)	25–28 (27)
	Quellon	QLN	49/48	03/18	172.1–238.2	193.3	5–9 (7)	11–12 (11)	16–21 (18)	7–10 (9)	25–29 (27)

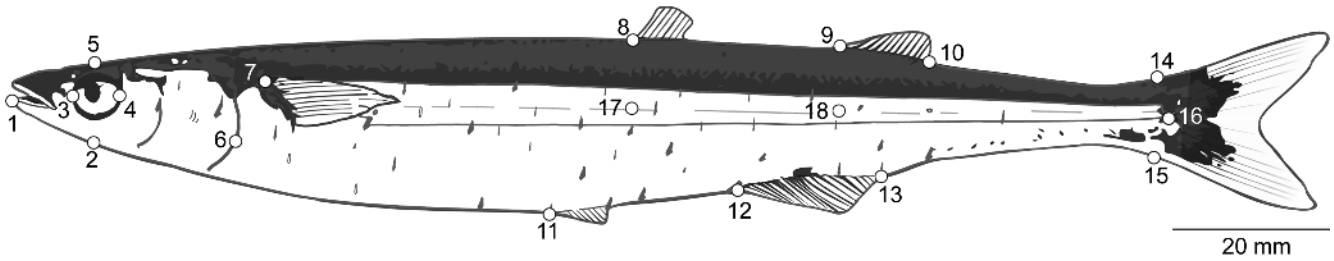

Fig. 2. Landmarks used: 1, anterior tip of the premaxilla; 2, ventral projection of the eye centre; 3, anterior edge of the eye; 4, posterior edge of the eye; 5, dorsal projection of the eye centre; 6, caudal extreme of opercula; 7, dorsal insertion of the pectoral fin; 8, anterior insertion of the first dorsal fin; 9, anterior insertion of the second dorsal fin; 10, posterior insertion of the second dorsal fin; 11, anterior insertion of the pelvic fin; 12, anterior insertion of the anal fin; 13, posterior insertion of the anal fin; 14, dorsal insertion of the caudal fin; 15, ventral insertion of the caudal fin; 16, end of the vertebral column; 17, projection of the landmark 8 onto the lateral line; 18, projection of the landmark 9 onto the lateral line

among locations and populations. After that, two canonical variate analyses (CVA) were carried out to evaluate the intra- and inter-population variation based on residuals. Both analyses were implemented using the R package Morpho (Schlager 2017). Thin-plane splines of extremely loaded individuals of each population from the consensus shape were built and pairwise comparisons of the average configuration of each population were conducted. Thin-plate splines were magnified 1.2 X to highlight differences. We used the R functions myTps, tps, and tps2d described by Claude (2008) to build all the thin-spline plates in this work.

Likewise, in meristic analysis, cross-validated classifications and a UPGMA tree were used to estimate the degree of association among locations and populations. To evaluate if meristic counts are related to the shape deformations, we performed multivariate regression analyses of the HEAD (total number of gill rakers (GRT) = GRU + GRL, on L1–L7) and FINS (RD1, RD2, RA, on L8–L13), separately.

We carried out multivariate regression analyses of meristic counts and residuals on mean values of the sea surface temperature (SST) and the surface chlorophyll-a (Chl-a) concentration to assess the relationship between meristic and geometric morphometric differences with the dissimilar upwelling intensity. We analysed data from two years before the sample collection, and with geographic coverage of 30' around the point of collection. These frames were considered to account for the minimum population doubling time (15 months) (http://www.fishbase.in) and the coastal distribution of the species. We downloaded these variables from the Nasa Earth Observation (NEO) website (http://www.neo.sci.gsfc.nasa.gov/) with a spatial resolution of 6' × 6'.

3. Results

All meristic counts had the same average value along latitude, except for RA and GRL (Table 1). CSCH locations had higher average counts in RA and GRL compared with the others. Significant statistical correlations ($P < 0.001$) were observed between TL and the meristic variables but with low to moderate Pearson's correlation coefficients ($0.09 < r < 0.36$), and were not confirmed in all locations, populations (Table A1) nor posterior ANOVAs (Table A2).

Pairwise MANOVAs of meristic counts showed significant differences among locations after Bonferroni sequential corrections (Rice 1989) (Table A3). SWDA of locations only selected RA, GRU, and GRL to derive the discriminant functions (DFs). DF1 accounted for 75.2% of the total variation, while DF2 explained 22.2%. The overall rate of cross-classification success for locations was 19.1% (Table A4).

Significant differences ($P < 0.001$) were detected in all pairwise comparisons of populations except when CP and SPNCH were contrasted ($P = 0.1758$). In the SWDA of populations with all variables except RD1, DF1 accounted for 82.6% of variance and DF2 for 16.5%. Correct cross-classification rate was 39.8% (Table 2). CSCH obtained the highest percentage of assignment, and most of its individuals were assigned to any of the CSCH locations with high probability reflecting a different variation in meristic counts (Fig. 3a). Furthermore, the divergence of CSCH samples and lack of differentiation among the others were displayed by the UPGMA tree (Fig. 4a). Although NP reached a moderate correct classification, all its individuals had low probabilities of being assigned to this place (Fig. 3a). Moderate values of misclassification among NP, CP, and SPNCH locations and

Table 2. Cross-classification values and percentages (in parenthesis) among populations of sea silverside (*Odontesthes regia*) based on stepwise discriminant analysis of meristic counts. Bold values indicate successfully classified individuals

Original population	Assigned population				Total
	NP	CP	SPNCH	CSCH	
NP	**62 (61.4)**	8 (7.9)	21 (20.8)	10 (9.9)	101 (100)
CP	125 (35.3)	**59 (16.7)**	129 (36.4)	41 (11.6)	354 (100)
SPNCH	61 (25.6)	37 (15.5)	**106 (44.5)**	34 (14.3)	238 (100)
CSCH	5 (3.9)	6 (4.7)	17 (13.4)	**99 (78.0)**	127 (100)

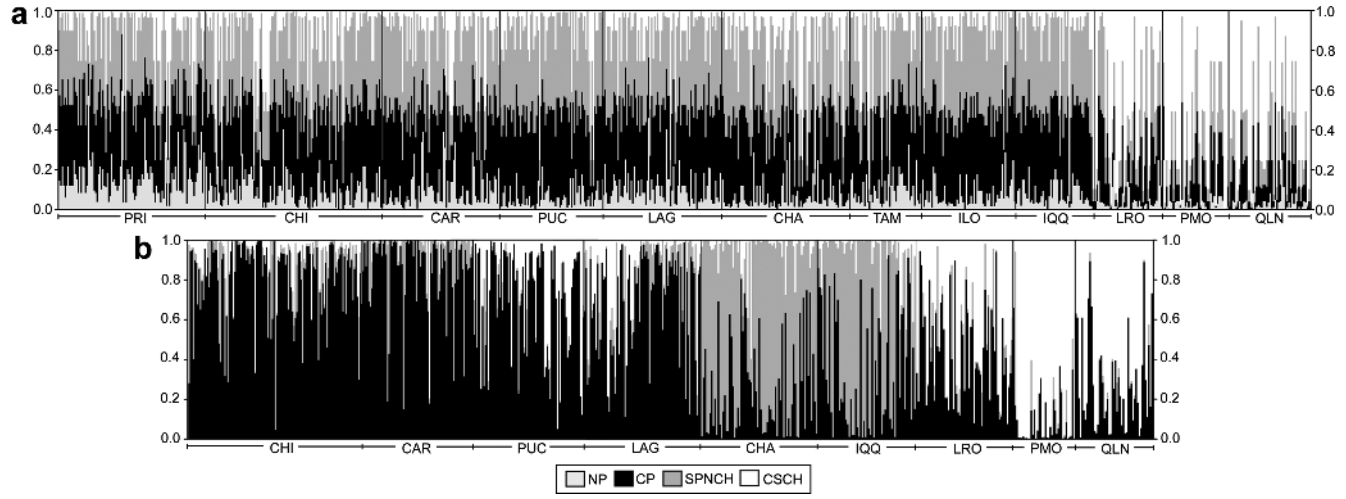

Fig. 3. Individual post-probabilities regarding assigned populations per location. A, based on stepwise discriminant analysis of meristic counts; B, based on canonical variate analysis of residuals from regression of Procrustes coordinates on log-transformed centroid size

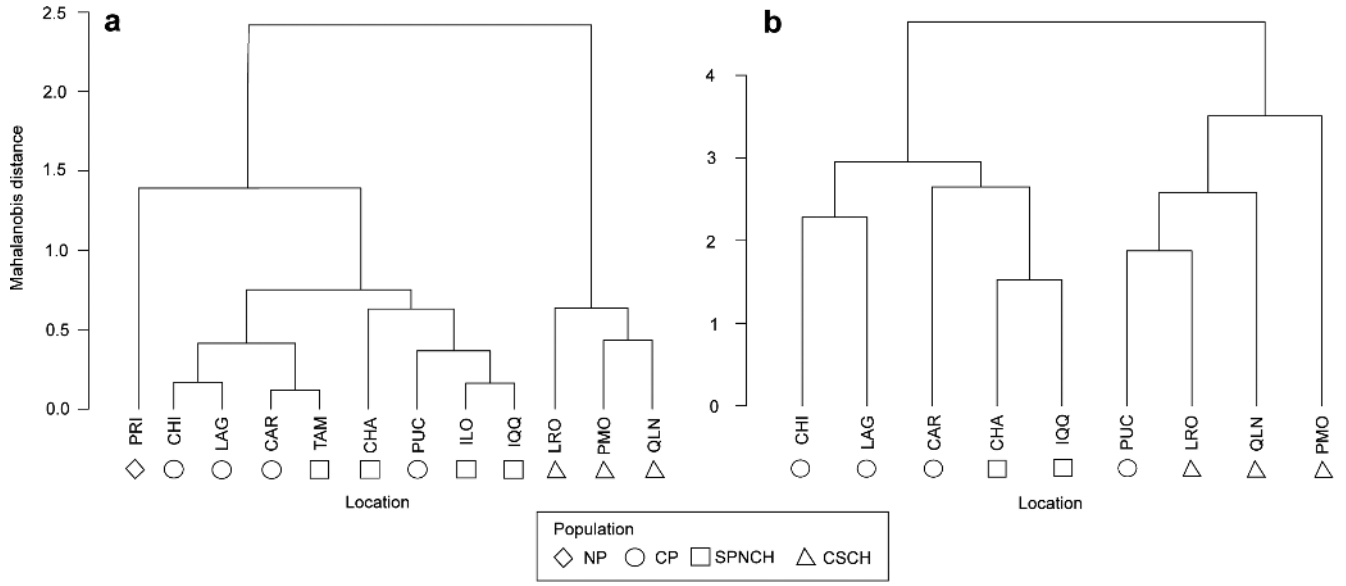

Fig. 4. UPGMA trees of Mahalanobis distances. A, estimated from meristic counts; B, estimated from residuals of the regression of Procrustes coordinates on log-transformed centroid size

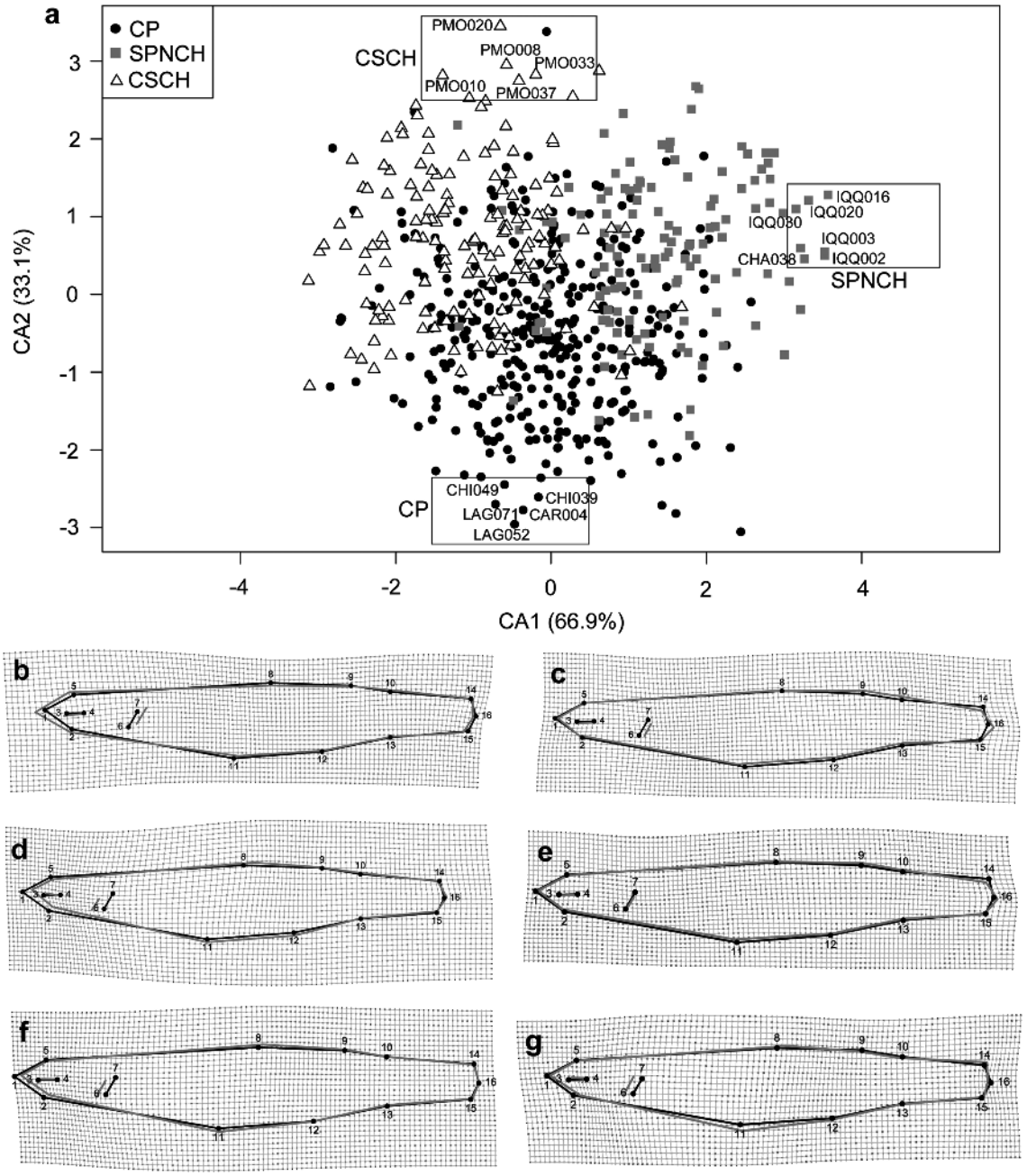

Fig. 5. Population differences by the distribution of CVA scores and thin-plate splines from residuals. a, CVA scores; b, CP deformation; c, SPNCH deformation; d, CSCH deformation; e, SPNCH mean configuration in relation to CP; f, CSCH in relation to CP; g, CSCH in relation to SPNCH. Grey lines indicate deformation in relation to the consensus shape used as reference

mixed probabilities in most of their individuals indicated a lack of differentiation among them (Table 2 and Fig. 3a).

Permutation tests of mean Procrustes distances showed significant comparisons considering Bonferroni sequential corrections (Table A3). CVA of locations retained four canonical axes (CAs) to account for 82.5% of the total variance. The overall assignment of individuals to their original locations was 65.3%. Cross-classification rates had moderate to high values (Table A5). IQQ had the most significant amount of misclassification (48.0%), while PMO reached the highest value of success assignment (94.9%).

Significant differences ($P < 0.001$) were found when pairwise

Table 3. Cross-classification values and percentages (in parenthesis) among populations of sea silverside (*Odontesthes regia*) based on canonical variate analysis of residuals from regression of Procrustes coordinates on log-transformed centroid size. Bold values indicate successfully classified individuals

Original population	Assigned population			Total
	CP	SPNCH	CSCH	
CP	**230 (64.6)**	54 (15.2)	72 (20.2)	356 (100)
SPNCH	23 (17.6)	**101 (77.1)**	7 (5.3)	131 (100)
CSCH	23 (15.4)	6 (4.0)	**120 (80.5)**	139 (100)

comparisons were performed among populations. In CVA of populations, the first canonical axis (CA1) explained 66.9% of all the variance, while the second axis (CA2) accounted for 33.1%. The plot of CVA scores separated individuals of the three populations but with moderate overlapping (Fig. 5a). CP specimens with negative loadings in both CAs had bigger heads due to longer snouts and bigger opercula (Fig. 5b). Positively loaded fish from SPNCH had the insertion of the dorsal and anal fin outward and inward deformed, respectively, meanwhile they presented bigger opercula in relation to the consensus configuration (Fig. 5c). Extremely loaded individuals of CSCH had smaller heads (smaller snouts and opercula), but their bodies were broader in the insertion of the pelvic fin compared to the consensus configuration (Fig. 5d).

The thin-plate spline of SPNCH in relation to CP average configuration did not show any noticeable difference (Fig. 5e). On the other hand, the average configuration of CSCH in relation to CP and SPNCH presented a smaller head (smaller snout and operculum) and a slightly broader body in the insertion of the pelvic fin (Fig. 5f and g).

CSCH had the highest rate of success under the cross-classification (Table 3). The correct assignment rate regarding populations was 70.9%. These high values of success classification were also supported by high probabilities of assigned individuals (Fig. 3b). The UPGMA tree based on residuals also separated CSCH locations from CP and SPNCH but clustered PUC near LRO (Fig. 4b) reflecting some degree of similarity.

HEAD and FINS sub-datasets indicated a significant correlation between shape deformations and meristic counts ($P < 0.001$). The SST and Chl-a mean values were significantly correlated ($P < 0.001$) with meristic counts and residuals from geometric morphometrics, respectively.

4. Discussion

This work is the first that highlights the influence of regions with different upwelling intensity along the HCS on the morphological variation of a coastal fish. Our study also supports the previously reported high adaptation of *Odontesthes* to the environment they inhabit (Beheregaray and Sunnucks 2001; Conte-Grand et al. 2015).

We observed that the increase of meristic counts in relation to the decrease of the sea surface temperature (SST) (RA and GRL in CSCH locations, Table 1; Fig. A2) follows Jordan's rule (McDowall 2008), which describes the opposite relationship between water temperatures and meristic counts in many fish species. Like in Dyer and Gosztonyi (1999), we also found an increase of GRT from north to south and a lack of latitudinal variation in the means of RD1 and RD2. Moreover, we found that the shape variations of the head were significantly correlated with GRT. GRT is inversely related with the size of food particles consumed (Hermida et al. 2005), and variations in the size of the head (e.g. snouts and opercula) are related to different prey consumption (Albertson and Kocher 2001). The presence of different prey-items for *O. regia* in CSCH is because this population is located after the biogeographic break reported at 30°S in the HCS for many invertebrate species (Camus 2001) that are the main items consumed by this sea silverside (Fierro et al. 2014).

The higher percentages of success classification in geometric morphometrics over meristic counts reflect a higher level of variation regarding the former data. This higher level of variation identified some samples from the same upwelling subsystem. Higher variation from morphometrics than from meristics also allowed for the discrimination of three-spined stickleback (*Gasterosteus aculeatus*) populations from different basins (Hermida et al. 2005). Nevertheless, the authors recommend that both morphometrics and meristics data are included to assess morphological variation since both data produce complementary information about the life history of species. Our findings after analysing meristic and geometric morphometric variations in each part of the HCS are discussed in the following paragraphs.

Variation in Northern Peru (NP)

Two interpretations can explain the variation in NP. First, NP contains an admixture of individuals from different locations rather than individuals from a unique population. These individuals might have migrated from CP, SPNCH, or both after their early development (Tables 2 and A4). This interpretation is partially supported by the sporadic fisheries landings of *O. regia* in PRI and ports located to the north of 6.5ºS (IMARPE data). Second but less likely, NP individuals could be partially exposed to similar conditions as CP and SPNCH during their early development (Swain et al. 2005) due to the continuous coastal upwelling intensity of the northern subsystem (Tables A6 and A7) (Montecino and Lange 2009), and the small contribution of equatorial subsurface currents in superficial waters around 5°S (Montes et al. 2010).

Variation in Central Peru (CP) and Southern Peru Northern Chile (SPNCH)

The short distance between most of the CP locations observed in the UPGMA trees (CHI, CAR, and LAG) (Fig. 4) might be related to the presence of prominent upwelling plumes (Tarazona and Arntz 2001). These locations are recognized as the most productive areas along the Peruvian sea but present lower levels of Chl-a concentration than PUC (Table A6) due to a deeper mixed layer in the plumes. In these upwelling plumes a stronger dilution effect and light limitation of Chl-a concentration (Echevin et al. 2008) create an opposite relationship between upwelling intensity and Chl-a concentration in this part of the HCS. Moreover, the presence of prominent upwelling plumes leads to the development of different phenotypic responses (Gaitán-Espitia et al. 2017) and predatory performances (Pulgar et al. 2013) in relation to places without upwelling, and reduces the level of connection among individuals from different populations (Cowen et al. 2000). Therefore, the lower level of connection could explain the moderate success assignment value of each location within CP (Table A5) despite their presence in the same upwelling subsystem.

The low level of variability between SPNCH locations in both analyses (Figs. 3 and 4) may be explained by the presence of a northward coastal flow (Chaigneau et al. 2013) and the lack of prominent upwelling plumes between 16°S to 22°S in this subsystem (Strub et al. 1998) that promotes more connection (Cowen et al. 2000) in SPNCH compared to CP.

The geometric morphometric results (Figs. 3b and 5, Table 3) support the growth of CP individuals under different conditions than those that prevail in SPNCH (Montecino and Lange 2009). These differences were not clear using meristic counts (Table 2, Fig. 3a), suggesting an early development of these populations in the austral winter under similar conditions (Grados et al. 2018), or less likely, the mixing of individuals in early development due to the presence of southward and northward coastal current flows from 11°S to 18°S (Chaigneau et al. 2013).

Variation in the Central and Southern Chile (CSCH)

The morphological differentiation in CSCH could be due to a lower-temperature exposition in the southern subsystem (Lindsey 1988; Montecino and Lange 2009), the existence of a unique long peak of spawning from July to October (Plaza et al. 2011) compared to the one additional peak off Peru in January (Gómez et al. 2006), and the dissimilar early developmental conditions (Swain et al. 2005; Montecino and Lange 2009). However, the similarity between LRO and PUC (Table A3; Figs. 3b and 4b) can be explained through the upwelling intensity levels, which are directly translated to similar high Chl-a concentrations in both places. As in most CP locations, LRO is also surrounded by seasonal prominent upwelling plumes (September–March) (Morales et al. 2007). However, the upwelling level of the Southern Humboldt area (i. e., CSCH) is lower (0.9×10^{-3} kg s^{-1} m^{-2}) than the level of upwelling of the Northern Humboldt area (1.1×10^{-3} kg s^{-1} m^{-2}) (Oyarzún and Brierley 2019). Consequently, in CSCH the dilution effect and light limitation for the Chl-a concentration are lower than in the CP upwelling plumes, producing as high Chl-a concentrations as a place under the strong permanent upwelling subsystem but without prominent upwelling plumes (e. g, PUC) (Table A6) (Henríquez et al. 2007; Echevin et al. 2008). Therefore, the upwelling intensity reflected in similar high Chl-a concentrations might explain the similar morphometric variation of PUC and LRO despite both belonging to different upwelling intensity subsystems.

In CSCH, PMO and QLN are more closely related compared to the other locations. PMO and QLN presented a more differentiated pattern of meristic and morphometric variation (Fig. 4 and Table A5) related to the chemical and physical features of the ISCh, which comprises a complex arrangement of semi-enclosed basins such as inlets, fjords, and estuaries (Zapata-Hernández et al. 2016). Based on their locations, this indicates that PMO individuals developed a purely estuarine form and grew in a productive environment with higher values of organic matter (Silva and Prego 2002), while

individuals in QLN had an intermediate marine-estuarine form because of the more dynamic interaction between ISCh and the HCS in this place (Zapata-Hernández et al. 2016).

Implications for fisheries management

Environmental conditions produce a rapid variation in morphometric and meristic characters. The assessment of these variations provides valuable information about the fast-local adaptation of species (Swain and Foote 1999) and how their life history characters might respond to different exploitation strategies (Hilborn and Waters 1992). Based on the presence of morphological differences between CP and SPNCH as consequence of the dissimilar upwelling intensity in the regions they belong to, we suggest that different management policies for these populations be considered. However, genetic studies that include nuclear variation (i.e., through microsatellite or SNPs) are necessary to complement our morphological analyses. These studies would provide information about the genetic connectivity of the populations considered here.

5. Conclusion

Based on meristic counts, individuals in Central-Southern Chile showed a higher number of gill rakers and a slight increase in the number of rays of the anal fin in relation to individuals from Peru and Northern Chile. Geometric morphometric results, however, showed noticeable deviations in the head and the insertion of the fins of specimens from Central Peru, Southern Peru-Northern Chile, and Central-Southern Chile. Both analyses revealed a phenotypic variation that is significantly correlated with SST and Chl-a concentration along the coastal distribution of the Humboldt Current System. These findings highlight the role that the heterogeneous spatial dynamics of the Humboldt Current System plays in the morphological differentiation of marine fish populations and provide valuable preliminary information for the stock management of *O. regia*.

Acknowledgements

This study was supported by the Japanese Government through the Ministry of Education, Culture, Sport, Science, and Technology (MEXT) and the Research Vice-rectorate of the Universidad Nacional Mayor de San Marcos (Code 151001077) in Lima, Peru. We would like to thank to all the IMARPE personnel who kindly helped with the collection of specimens from Peru.

References

Albertson RC, Kocher TD (2001) Assessing morphological differences in an adaptive trait: A landmark-based morphometric approach. J Exp Zool **289**:385–403. doi:10.1002/jez.1020

Beheregaray LB, Levy JA (2000) Population genetics of the silverside *Odontesthes argentinensis* (Teleostei, Atherinopsidae): Evidence for speciation in an estuary of Southern Brazil. Copeia **2000**(2):441–447. doi:10.1643/0045-8511(2000)000[0441:PGOTSO]2.0.CO;2

Beheregaray LB, Sunnucks P (2001) Fine-scale genetic structure, estuarine colonization and incipient speciation in the marine silverside fish *Odontesthes argentinensis*. Mol Ecol **10**(12):2849–2866. doi:10.1046/j.1365-294X.2001.t01-1-01406.x

Booke HE (1981) The conundrum of the stock concept—Are nature and nurture definable in fishery science? Can J Fish Aquat Sci **38**(12):1479–1480. doi:10.1139/f81-200

Camus PA (2001) Biogeografía marina de Chile continental. Rev Chil Hist Nat **74**:587–617

Chaigneau A, Dominguez N, Eldin G, Vasquez L, Flores R, Grados C, Echevin V (2013) Near-coastal circulation in the Northern Humboldt Current System from shipboard ADCP data. J Geophys Res-Oceans **118**(10):5251–5266. doi:10.1002/jgrc.20328

Chavez FP, Bertrand A, Guevara-Carrasco R, Soler P, Csirke J (2008) The northern Humboldt Current System: Brief history, present status and a view towards the future. Prog Oceanogr **79**(2):95–105. doi:10.1016/j.pocean.2008.10.012

Claude J (2008) Modern morphometrics based on configurations of landmarks. In: Claude J (ed) Morphometrics with R. Springer, New York, pp 131–202

Conte-Grand C, Sommer J, Ortí G, Cussac V (2015) Populations of *Odontesthes* (Teleostei: Atheriniformes) in the Andean region of Southern South America: Body shape and hybrid individuals. Neotrop Ichthyol **13**(1):137–150. doi:10.1590/1982-0224-20130094

Cowen RK, Lwiza KMM, Sponaugle S, Paris CB, Olson DB (2000) Connectivity of marine populations: Open or closed? Science **287**:857–859. doi:10.1126/science.287.5454.857

Dyer BS (2006) Systematic revision of the South American silversides (Teleostei, Atheriniformes). Biocell **30**(1):69–88

Dyer BS, Gosztonyi AE (1999) Phylogenetic revision of the South American subgenus *Austromenidia* Hubbs, 1918 (Teleostei, Atherinopsidae, *Odontesthes*) and a study of meristic variation. Rev Biol Mar Oceanogr **34**:211–232

Echevin V, Aumont O, Ledesma J, Flores G (2008) The seasonal cycle of surface chlorophyll in the Peruvian upwelling system: A modelling study. Prog Oceanogr **79**(2):167–176. doi:10.1016/

j.pocean.2008.10.026
Fierro P, Bertran C, Martinez D, Valdovinos C, Vargas-Chacoff L (2014) Ontogenic and temporal changes in the diet of the Chilean silverside *Odontesthes regia* (Atherinidae) in southern Chile. Cah Biol Mar **55**:323–332
Gaitán-Espitia JD, Villanueva PA, Lopez J, Torres R, Navarro JM, Bacigalupe LD (2017) Spatio-temporal environmental variation mediates geographical differences in phenotypic responses to ocean acidification. Biol Lett **13**:20160865. doi:10.1098/rsbl.2016.0865
García G, Ríos N, Gutiérrez V, Varela JG, Fernández CB, Pardo BG, Portela PM (2014) Promiscuous speciation with gene flow in silverside fish genus *Odontesthes* (Atheriniformes, Atherinopsidae) from South Western Atlantic Ocean basins. PloS One **9**(8):e104659. doi:10.1371/journal.pone.0104659
Gómez AC, Perea Á, Williams de Castro M (2006) Reproductive aspects in the silverside *Odontesthes regia regia* (Humboldt 1821) from Pisco, Peru, during 1996–1997 and May–July, 2002, related to its conservation. Ecol Apl **5**(1–2):141–147
González-Castro M, Rosso JJ, Mabragaña E, Díaz de Astarloa JM (2016) Surfing among species, populations and morphotypes: Inferring boundaries between two species of new world silversides (Atherinopsidae). C R Biol **339**(1):10–23. doi:10.1016/j.crvi.2015.11.004
Grados C, Chaigneau A, Echevin V, Dominguez N (2018) Upper ocean hydrology of the Northern Humboldt Current System at seasonal, interannual and interdecadal scales. Prog Oceanogr **165**:123–144. doi:10.1016/j.pocean.2018.05.005
Haye PA, Salinas P, Acuña E, Poulin E (2010) Heterochronic phenotypic plasticity with lack of genetic differentiation in the southeastern Pacific squat lobster *Pleuroncodes monodon*. Evol Dev **12**:628–634. doi:10.1111/j.1525-142X.2010.00447.x
Heino M (2014) Quantitative traits. In: Cadrin SX, Kerr LA, Mariani S (eds) Stock identification methods: Applications in fishery science. Academic Press, San Diego, pp 59–76
Henríquez LA, Daneri G, Muñoz CA, Montero P, Veas R, Palma AT (2007) Primary production and phytoplanktonic biomass in shallow marine environments of central Chile: Effect of coastal geomorphology. Estuar Coast Shelf S **73**(1):137–147. doi:10.1016/j.ecss.2006.12.013
Hermida M, Fernández JC, Amaro R, Miguel ES (2005) Morphometric and meristic variation in Galician threespine stickleback populations, northwest Spain. Environ Biol Fish **73**:189–200. doi:10.1007/s10641-005-2262-0
Hilborn R, Walters CJ (1992) Quantitative fisheries stock assessment: Choice, dynamics and uncertainty. Chapman and Hall, New York, 570 p
Lindsey CC (1988) 3 factors controlling meristic variation. In: Hoar WS, Randall DJ (eds) Fish physiology. Academic Press, Cambridge, pp 197–274
McDowall RM (2008) Jordan's and other ecogeographical rules, and the vertebral number in fishes. J Biogeogr **35**:501–508. doi:10.1111/j.1365-2699.2007.01823.x
Montecino V, Lange CB (2009) The Humboldt Current System: Ecosystem components and processes, fisheries, and sediment studies. Prog Oceanogr **83**(1):65–79. doi:10.1016/j.pocean.2009.07.041
Montes I, Colas F, Capet X, Schneider W (2010) On the pathways of the equatorial subsurface currents in the eastern equatorial Pacific and their contributions to the Peru-Chile Undercurrent. J Geophys Res-Oceans **115**(C9):C09003. doi:10.1029/2009JC005710
Morales CE, González HE, Hormazabal SE, Yuras G, Letelier J, Castro LR (2007) The distribution of chlorophyll-a and dominant planktonic components in the coastal transition zone off Concepción, central Chile, during different oceanographic conditions. Prog Oceanogr **75**(3):452–469. doi:10.1016/j.pocean.2007.08.026
Murta AG, Pinto AL, Abaunza P (2008) Stock identification of horse mackerel (*Trachurus trachurus*) through the analysis of body shape. Fish Res **89**(2):152–158. doi:10.1016/j.fishres.2007.09.026
Oyarzún D, Brierley CM (2019) The future of coastal upwelling in the Humboldt current from model projections. Clim Dynam **52**:599–615. doi:10.1007/s00382-018-4158-7
Plaza G, Espejo V, Almanza V, Claramunt G (2011) Female reproductive biology of the silverside *Odontesthes regia*. Fish Res **111**(1):31–39. doi:10.1016/j.fishres.2011.06.009
Pulgar J, Poblete E, Alvarez M, Morales JP, Aranda B, Aldana M, Pulgar VM (2013) Can upwelling signals be detected in intertidal fishes of different trophic levels? J Fish Biol **83**:1407–1415. doi:10.1111/jfb.12220
Rice WR (1989) Analyzing tables of statistical tests. Evolution **43**:223–225. doi:10.1111/j.1558-5646.1989.tb04220.x
Rohlf FJ (2017) tpsDig, digitize landmarks and outlines, version 2.31. Department of Ecology and Evolution, State University of New York at Stony Brook. https://life.bio.sunysb.edu/morph/Accesed 20 Jun 2018
Rohlf FJ (2018) tpsUtil, file utility program. version 1.78. Department of Ecology and Evolution, State University of New York at Stony Brook. https://life.bio.sunysb.edu/morph/soft-utility.html Accesed 20 Jun 2018
Rohlf FJ, Slice D (1990) Extensions of the procrustes method for the optimal superimposition of landmarks. Syst Zool **39**(1):40–59. doi:10.2307/2992207
Sathyendranath S, Platt T (2001) Primary production distribution. In: Steele JH (ed) Encyclopedia of ocean sciences. Academic Press, New York, pp 572–577
Schlager S (2017) Morpho and Rvcg – Shape analysis in R: R-Packages for geometric morphometrics, shape analysis and surface manipulations. In: Zheng G, Li S, Székely G (eds) Statistical shape and deformation analysis. Academic Press, New York, pp 217–256

Silva N, Prego R (2002) Carbon and nitrogen spatial segregation and stoichiometry in the surface sediments of Southern Chilean inlets (41°–56°S). Estuar Coast Shelf S **55**(5):763–775. doi: 10.1006/ecss.2001.0938

Silva N, Rojas N, Fedele A (2009) Water masses in the Humboldt Current System: Properties, distribution, and the nitrate deficit as a chemical water mass tracer for equatorial water off Chile. Deep-Sea Res Pt II **56**:992–1008. doi:10.1016/j.dsr2.2008.12.013

Strub PT, Mesías J, Montecino V, Rutllant J, Salinas S (1998) Coastal ocean circulation off western South America. In: Brink KH, Robinson AR (eds) The sea. Wiley & Sons, Hoboken, pp 273–313

Swain DP, Foote CJ (1999) Stocks and chameleons: The use of phenotypic variation in stock identification. Fish Res **43**(1):113–128. doi:10.1016/S0165-7836(99)00069-7

Swain DP, Hutchings JA, Foote CJ (2005) Environmental and genetic influences on stock identification characters. In: Cadrin SX, Friedland KD, Waldman JR (eds) Stock identification methods. Academic Press, Burlington, pp 45–85

Tarazona J, Arntz W (2001) The Peruvian coastal upwelling system. In: Seeliger U, Kjerfve B (eds) Coastal marine ecosystems of Latin America. Springer, Berlin, pp 229–244

Vega MA, Rocha FJ, Guerra A, Osorio C (2002) Morphological differences between the Patagonian squid Loligo gahi populations from the Pacific and Atlantic Oceans. B Mar Sci **71**(2):903–913

Zapata-Hernández G, Sellanes J, Thiel M, Henríquez C, Hernández S, Fernández JCC, Hajdu E (2016) Community structure and trophic ecology of megabenthic fauna from the deep basins in the Interior Sea of Chiloé, Chile (41–43°S). Cont Shelf Res **130**:47–67. doi:10.1016/j.csr.2016.10.002

Appendix

Table A1. Pearson's correlation (r) and its significance (P) between each meristic count on the total length. RD1 = radius of the first dorsal fin, RD2 = radius of the second dorsal fin, RA= radius of the anal fin, GRU = gill rakers of the upper branch of the first gill arch from the left side, GRL = gill rakers of the lower branch of the first gill arch from the left side. PRI = Puerto Rico, CHI = Chimbote, CAR = Carquin, PUC = Pucusana, LAG = Lagunilla, CHA = Chala, TAM = Tambo, IQQ = Iquique, LRO = Lo Rojas, PMO = Puerto Montt, QLN = Quellon

Location	Meristic count									
	RD1		RD2		RA		GRU		GRL	
	r	P	r	P	r	P	r	P	r	P
PRI	0.115	0.250	0.087	0.385	-0.012	0.906	0.088	0.382	0.191	0.056
CHI	-0.008	0.933	0.109	0.235	0.096	0.294	0.231	0.011	0.086	0.350
CAR	0.196	0.080	-0.052	0.647	0.054	0.630	0.043	0.700	-0.036	0.746
PUC	0.077	0.524	0.155	0.197	0.117	0.330	0.099	0.414	0.048	0.692
LAG	-0.082	0.468	0.110	0.327	-0.104	0.356	0.196	0.079	0.110	0.328
CHA	0.206	0.064	0.154	0.166	-0.007	0.953	0.194	0.081	0.195	0.079
TAM	-0.208	0.165	0.011	0.944	-0.154	0.307	0.302	0.041	0.241	0.107
ILO	0.078	0.552	-0.085	0.517	-0.165	0.208	0.077	0.556	0.273	0.035
IQQ	0.112	0.441	-0.055	0.705	0.094	0.517	0.204	0.155	0.013	0.930
LRO	-0.068	0.675	0.313	0.049	0.122	0.455	-0.002	0.990	0.009	0.955
PMO	0.278	0.087	0.351	0.028	0.446	0.004	-0.136	0.408	0.361	0.024
QLN	-0.256	0.079	-0.226	0.123	0.382	0.007	0.062	0.678	0.279	0.055
All	0.091	0.009	0.141	0.000	0.154	0.000	0.36	0.000	0.295	0.000

Table A2. ANOVA tests (F) of the total length and their significance (P) considering each meristic count as a factor. RD1 = radius of the first dorsal fin, RD2 = radius of the second dorsal fin, RA= radius of the anal fin, GRU = gill rakers of the upper branch of the first gill arch from the left side, GRL = gill rakers of the lower branch of the first gill arch from the left side. PRI = Puerto Rico, CHI = Chimbote, CAR = Carquin, PUC = Pucusana, LAG = Lagunilla, CHA = Chala, TAM = Tambo, IQQ = Iquique, LRO = Lo Rojas, PMO = Puerto Montt, QLN = Quellon

Location	Meristic count									
	RD1		RD2		RA		GRU		GRL	
	F	P	F	P	F	P	F	P	F	P
PRI	0.587	0.625	0.286	0.835	0.272	0.895	0.489	0.691	1.183	0.322
CHI	0.273	0.845	0.803	0.450	0.771	0.546	2.548	0.059	0.611	0.746
CAR	1.063	0.370	0.399	0.672	0.100	0.982	0.405	0.749	0.618	0.739
PUC	2.109	0.090	1.690	0.192	0.515	0.674	0.682	0.509	0.909	0.505
LAG	0.603	0.615	0.857	0.494	1.696	0.160	4.858	0.004	0.434	0.854
CHA	1.319	0.270	1.734	0.183	1.090	0.368	2.061	0.112	1.284	0.280
TAM	1.806	0.161	0.390	0.679	0.811	0.526	4.427	0.041	0.527	0.808
ILO	1.568	0.207	0.287	0.752	1.965	0.113	0.691	0.561	1.530	0.170
IQQ	0.823	0.488	2.073	0.137	0.981	0.410	0.904	0.446	0.331	0.935
LRO	1.319	0.282	1.353	0.273	0.661	0.623	0.607	0.551	1.472	0.225
PMO	2.652	0.064	2.134	0.113	2.354	0.073	0.357	0.838	2.552	0.071
QLN	0.818	0.521	2.470	0.123	2.324	0.060	0.366	0.778	3.179	0.023

Table A3. P-values of pairwise location comparisons from multivariate analysis of variance (MANOVA) of meristic counts (above diagonal) and permuation tests of mean Procrustes distances (below diagonal). Bold values indicate statistical significance after Bonferroni sequential corrections

Population	Location	CHI	CAR	PUC	LAG	CHA	TAM	ILO	IQQ	LRO	PMO	QLN
NP	PRI	**0.000**	**0.000**	**0.000**	**0.0005**	**0.000**	0.01	**0.000**	**0.000**	**0.000**	**0.000**	**0.000**
CP	CHI		0.175	0.0002	0.3024	**0.000**	0.2613	0.0442	0.2614	**0.000**	**0.000**	**0.000**
	CAR	**< 0.0001**		0.0007	0.112	**0.0002**	0.8347	0.221	0.5616	**0.000**	**0.000**	**0.000**
	PUC	**< 0.0001**	**< 0.0001**		0.0014	**0.0002**	0.0092	0.0549	0.0232	**0.000**	**0.000**	**0.000**
	LAG	**< 0.0001**	**< 0.0001**	**< 0.0001**		**0.000**	0.6634	0.0058	0.0223	**0.000**	**0.000**	**0.000**
SPNCH	CHA	**< 0.0001**	**< 0.0001**	**< 0.0001**	**< 0.0001**		**0.0004**	**0.0006**	**0.0005**	**0.000**	**0.000**	**0.000**
	TAM	-	-	-	-	-		0.0908	0.2465	**0.000**	**0.000**	**0.000**
	ILO	-	-	-	-	-	-		0.8947	**0.000**	**0.000**	**0.000**
	IQQ	**< 0.0001**	**< 0.0001**	**< 0.0001**	**< 0.0001**	0.231	-	-		**0.000**	**0.000**	**0.000**
CSCH	LRO	**< 0.0001**	**< 0.0001**	**0.0052**	**< 0.0001**	**< 0.0001**	-	-	**< 0.0001**		0.123	0.4699
	PMO	**< 0.0001**	**< 0.0001**	**< 0.0001**	**< 0.0001**	**< 0.0001**	-	-	**< 0.0001**	**< 0.0001**		0.3876
	QLN	**< 0.0001**	**< 0.0001**	**< 0.0001**	**< 0.0001**	**< 0.0001**	-	-	**< 0.0001**	**< 0.0001**	**< 0.0001**	

Table A4. Cross-classification values and percentages of assignment (in parenthesis) among locations based on SWDA of meristic counts. Bold values indicate successfully classified individuals

Original location	Assigned location												Total
	PRI	CHI	CAR	PUC	LAG	CHA	TAM	ILO	IQQ	LRO	PMO	QLN	
PRI	**58(57.4)**	3(3.0)	3(3.0)	4(4.0)	0(0.0)	0(0.0)	12(11.9)	1(1.0)	0(0.0)	17(16.8)	3(3.0)	0(0.0)	101(100)
CHI	40(33.1)	**11(9.1)**	4(3.3)	23(19.0)	1(0.8)	6(5.0)	5(4.1)	3(2.5)	0(0.0)	17(14.0)	5(4.1)	6(5.0)	121(100)
CAR	24(29.6)	8(9.9)	**4(4.9)**	19(23.5)	0(0.0)	3(3.7)	7(8.6)	3(3.7)	0(0.0)	7(8.6)	3(3.7)	3(3.7)	81(100)
PUC	9 12.7)	6(8.5)	2(2.8)	**25(35.2)**	0(0.0)	10(14.1)	6(8.5)	5(7.0)	0(0.0)	4(5.6)	0(0.0)	4(5.6)	71(100)
LAG	29(35.8)	10(12.3)	5(6.2)	13(16.0)	**0(0.0)**	6(7.4)	4(4.9)	3(3.7)	0(0.0)	9(11.1)	0(0.0)	2(2.5)	81(100)
CHA	17(20.7)	3(3.7)	2(2.4)	22(26.8)	0(0.0)	**15(18.3)**	1(1.2)	2(2.4)	0(0.0)	10(12.2)	2(2.4)	8(9.8)	82(100)
TAM	15(32.6)	2(4.3)	2(4.3)	5(10.9)	0(0.0)	3(6.5)	**6(13.0)**	3(6.5)	0(0.0)	6(13.0)	0(0.0)	4(8.7)	46(100)
ILO	13(21.7)	2(3.3)	4(6.7)	15(25.0)	0(0.0)	13(21.7)	8(13.3)	**2(3.3)**	0(0.0)	3(5.0)	0(0.0)	0(0.0)	60(100)
IQQ	14(28.0)	4(8.0)	3(6.0)	8(16.0)	0(0.0)	9(18.0)	4(8.0)	4(8.0)	**0(0.0)**	2(4.0)	1(2.0)	1(2.0)	50(100)
LRO	3(7.5)	2(5.0)	0(0.0)	2(5.0)	0(0.0)	5(12.5)	0(0.0)	1(2.5)	0(0.0)	**6(15.0)**	9(22.5)	12(30.0)	40(100)
PMO	1(2.6)	1(2.6)	3(7.7)	0(0.0)	0(0.0)	2(5.1)	0(0.0)	0(0.0)	0(0.0)	9(23.1)	**12(30.8)**	11(28.2)	39(100)
QLN	1(2.1)	1(2.1)	0(0.0)	3(6.3)	0(0.0)	0(0.0)	0(0.0)	0(0.0)	0(0.0)	13(27.1)	12(25.0)	**18(37.5)**	48(100)

Table A5. Cross-classification values and percentages (in parenthesis) among locations as revealed by CVAs of residuals from the regression of shape on centroid size. Bold values indicate successfully classified individuals

Original location	Assigned location									Total
	CHI	CAR	PUC	LAG	CHA	IQQ	LRO	PMO	QLN	
CHI	**74(61.2)**	5(4.1)	8(6.6)	13(10.7)	6(5.0)	4(3.3)	9(7.4)	1(0.8)	1(0.8)	121(100)
CAR	7(9.1)	**55(71.4)**	4(5.2)	3(3.9)	5(6.5)	2(2.6)	1(1.3)	0(0.0)	0(0.0)	79(100)
PUC	4(5.2)	0(0.0)	**46(59.7)**	2(2.6)	2(2.6)	0(0.0)	11(14.3)	1(1.3)	11(14.3)	76(100)
LAG	4(4.9)	2(2.5)	2(2.5)	**47(58.0)**	6(7.4)	3(3.7)	12(14.8)	2(2.5)	3(3.7)	81(100)
CHA	8(9.9)	3(3.7)	2(2.5)	4(4.9)	**51(63.0)**	9(11.1)	2(2.5)	1(1.2)	1(1.2)	82(100)
IQQ	3(6.0)	3(6.0)	2(2.0)	7(14.0)	7(14.0)	**26(52.0)**	3(6.0)	0(0.0)	0(0.0)	50(100)
LRO	2(3.3)	1(1.6)	10(16.4)	4(6.6)	1(1.6)	1(3.6)	**39(63.9)**	0(0.0)	3(4.9)	61(100)
PMO	0(0.0)	0(0.0)	0(0.0)	0(0.0)	1(2.6)	0(0.0)	1(2.6)	**37(94.9)**	0(0.0)	39(100)
QLN	0(0.0)	0(0.0)	5(10.2)	2(4.1)	0(0.0)	0(0.0)	0(0.0)	2(4.1)	**40(81.6)**	49(100)

Table A6. Monthly mean surface chlorophyll-a concentration (mgChl-a/m^3) around each sample location in the last two years before the collection. PRI = Puerto Rico, TAM = Tambo, CHI = Chimbote, CAR = Carquin, PUC = Pucusana, LAG = Lagunilla, CHA = Chala, IQQ = Iquique, LRO = Lo Rojas, PMO = Puerto Montt, QLN = Quellon

Year		2015					2018					
Month	PRI	TAM	ILO	Month	CHI	CAR	PUC	LAG	CHA	IQQ	LRO	PMO	QLN
Jan-13	3.87	2.54	3.36	Jan-16	4.24	8.22	9.73	5.56	2.26	1.80	10.55	12.18	7.40
Feb-13	4.60	7.07	5.53	Feb-16	4.88	5.53	8.28	7.98	1.80	3.04	9.19	11.48	6.91
Mar-13	4.21	5.58	5.98	Mar-16	5.84	6.20	10.11	9.01	4.21	3.39	8.96	8.12	3.54
Apr-13	1.92	7.29	7.83	Apr-16	6.22	6.99	12.69	6.51	1.76	2.35	6.27	5.29	1.81
May-13	2.23	5.23	6.08	May-16	6.65	6.40	10.36	7.10	3.17	1.73	3.32	12.36	1.83
Jun-13	1.30	3.05	5.62	Jun-16	2.75	2.30	2.86	6.01	1.60	1.40	3.87	9.83	2.20
Jul-13	1.28	1.92	10.91	Jul-16	2.01	3.19	3.34	5.20	1.20	2.24	2.73	14.77	1.19
Aug-13	1.51	5.31	4.44	Aug-16	2.50	4.63	2.59	4.82	2.08	1.30	4.66	4.08	1.59
Sep-13	1.92	6.90	7.85	Sep-16	5.47	3.08	7.26	8.61	3.11	3.28	7.42	10.96	2.67
Oct-13	1.52	10.64	10.80	Oct-16	11.48	4.74	5.85	8.01	6.21	1.39	13.79	6.13	2.36
Nov-13	1.26	10.27	5.14	Nov-16	13.45	8.15	15.03	6.97	12.05	3.49	12.83	10.80	6.12
Dec-13	3.42	7.83	7.52	Dec-16	9.45	12.26	19.42	13.36	4.03	2.85	13.05	4.85	14.73
Jan-14	5.92	6.83	4.70	Jan-17	8.17	6.38	5.48	6.13	4.25	2.27	13.01	3.39	2.47
Feb-14	5.99	11.47	6.17	Feb-17	4.98	13.72	12.86	7.41	5.62	6.03	10.47	9.59	1.14
Mar-14	5.01	6.19	5.85	Mar-17	3.50	12.91	12.13	11.37	3.09	6.30	10.12	6.77	2.65
Apr-14	4.49	4.83	4.59	Apr-17	9.38	11.55	10.27	5.99	2.77	7.11	4.55	5.90	2.97
May-14	2.37	3.17	5.26	May-17	2.97	3.74	6.38	6.57	1.98	3.62	3.83	6.11	1.87
Jun-14	2.52	4.39	5.50	Jun-17	2.94	1.73	0.91	3.57	1.22	1.29	3.07	0.44	1.41
Jul-14	2.51	5.26	2.84	Jul-17	1.61	1.89	4.03	4.10	1.38	0.82	2.81	2.92	1.67
Aug-14	1.68	14.34	4.96	Aug-17	1.56	1.90	1.39	3.13	0.90	1.13	2.78	0.42	1.46
Sep-14	2.19	2.75	3.57	Sep-17	3.49	2.74	9.97	2.79	1.55	3.96	6.64	10.99	1.79
Oct-14	3.47	6.56	10.55	Oct-17	3.79	2.19	9.86	8.89	2.98	2.00	10.09	10.05	1.21
Nov-14	3.69	2.65	2.30	Nov-17	10.14	15.36	6.59	6.01	9.22	2.74	11.14	4.46	3.87
Dec-14	3.68	3.68	3.82	Dec-17	7.65	4.79	5.10	2.98	3.03	2.24	7.82	4.35	3.02
Jan-15	4.17	5.75	2.89	Jan-18	9.02	9.56	8.61	6.71	11.42	3.78	14.74	4.12	4.62
Feb-15	4.34	3.11	5.82	Feb-18	6.53	4.34	9.42	3.45	2.55	4.10	5.80	4.10	3.44
Mar-15	8.30	4.19	3.22	Mar-18	13.04	6.05	6.67	6.17	3.50	2.43	5.96	4.22	1.33
Mean	3.31	5.88	5.67	Mean	6.06	6.32	8.04	6.46	3.66	2.89	7.76	6.99	3.23
Sum	92.7	164.9	158.8		169.7	176.9	225.2	180.9	102.6	80.9	217.2	195.7	90.5

Table A7. Monthly mean and average sea surface temperature (SST) around each sample location in the last two years before the collection. PRI = Puerto Rico, TAM = Tambo, CHI = Chimbote, CAR = Carquin, PUC = Pucusana, LAG = Lagunilla, CHA = Chala, IQQ = Iquique, LRO = Lo Rojas, PMO = Puerto Montt, QLN = Quellon

Year		2015					2018					
Month	PRI	TAM	ILO	Month	CHI	CAR	PUC	LAG	CHA	IQQ	LRO	PMO	QLN
Jan-13	20.92	22.04	22.03	Jan-16	23.17	23.12	23.13	22.58	22.48	23.89	17.78	17.67	13.95
Feb-13	21.25	22.62	22.74	Feb-16	24.21	23.38	23.83	22.68	22.52	23.74	16.02	16.20	13.55
Mar-13	22.20	20.65	21.40	Mar-16	23.26	22.53	23.00	21.99	21.27	21.67	14.76	14.41	12.44
Abr-13	19.95	20.43	20.89	Apr-16	21.46	21.24	21.40	20.45	19.92	20.76	14.59	13.01	11.92
May-13	18.89	17.91	18.80	May-16	20.14	19.84	20.07	19.47	18.70	20.13	14.53	12.18	11.42
Jun-13	18.02	18.03	18.28	Jun-16	18.89	18.92	18.87	17.91	17.98	18.89	13.34	11.22	10.80
Jul-13	17.37	17.74	17.80	Jul-16	18.81	17.92	18.29	17.51	17.85	18.28	11.90	10.71	10.25
Ago-13	17.16	16.79	17.35	Aug-16	18.07	17.06	17.53	16.90	16.76	18.30	12.62	10.68	10.09
Set-13	17.44	16.94	17.76	Sep-16	18.47	17.57	17.52	16.85	17.28	18.60	12.94	11.51	10.77
Oct-13	17.34	17.33	17.82	Oct-16	18.51	18.21	18.28	17.76	17.62	19.27	13.53	13.48	11.33
Nov-13	19.08	19.41	20.09	Nov-16	19.14	18.75	19.37	18.61	18.91	20.20	13.87	14.31	12.09
Dic-13	19.86	20.47	21.00	Dec-16	19.36	19.78	20.26	19.39	19.56	21.17	15.02	16.40	12.66
Ene-14	22.61	22.15	22.48	Jan-17	21.88	21.08	21.73	20.90	21.49	24.45	15.07	17.99	13.33
Feb-14	21.10	20.73	21.63	Feb-17	26.05	23.71	23.46	22.27	21.98	21.43	15.63	17.29	13.37
Mar-14	21.75	20.62	20.95	Mar-17	27.35	23.81	24.10	22.17	21.08	20.72	15.46	15.21	12.85
Abr-14	21.02	20.62	21.84	Apr-17	22.19	21.16	21.69	20.10	20.40	20.04	15.35	13.82	12.30
May-14	22.55	20.32	20.59	May-17	20.64	19.94	20.24	19.95	19.82	20.30	14.73	12.14	11.67
Jun-14	21.63	18.98	19.14	Jun-17	19.78	19.11	19.47	18.37	19.30	19.53	13.37	11.02	11.03
Jul-14	19.50	16.79	18.16	Jul-17	19.77	18.83	18.04	18.08	17.38	17.64	12.86	10.53	10.40
Ago-14	18.29	16.43	17.28	Aug-17	17.98	17.58	17.55	16.09	16.16	17.96	12.13	10.39	10.03
Set-14	17.68	17.65	17.50	Sep-17	17.60	17.43	16.86	15.66	15.94	17.79	12.38	10.74	10.33
Oct-14	18.75	18.83	19.07	Oct-17	16.86	16.73	16.88	16.18	16.73	18.57	12.25	11.63	10.57
Nov-14	18.70	19.46	20.76	Nov-17	18.30	18.24	18.43	17.46	17.49	19.20	14.04	13.76	11.58
Dic-14	19.21	20.03	20.51	Dec-17	18.36	18.61	18.99	19.00	19.94	20.93	14.53	15.36	11.81
Ene-15	21.16	21.82	22.46	Jan-18	20.22	20.04	20.84	20.13	20.01	20.87	14.42	16.45	12.67
Feb-15	22.31	21.89	22.72	Feb-18	20.28	20.62	20.98	20.22	21.97	22.10	15.15	16.43	12.41
Mar-15	23.43	23.09	22.82	Mar-18	19.98	19.83	20.32	19.47	19.56	21.44	14.59	14.49	11.91
Mean	19.97	19.62	20.14	Mean	20.40	19.82	20.04	19.19	19.26	20.29	14.18	13.67	11.76

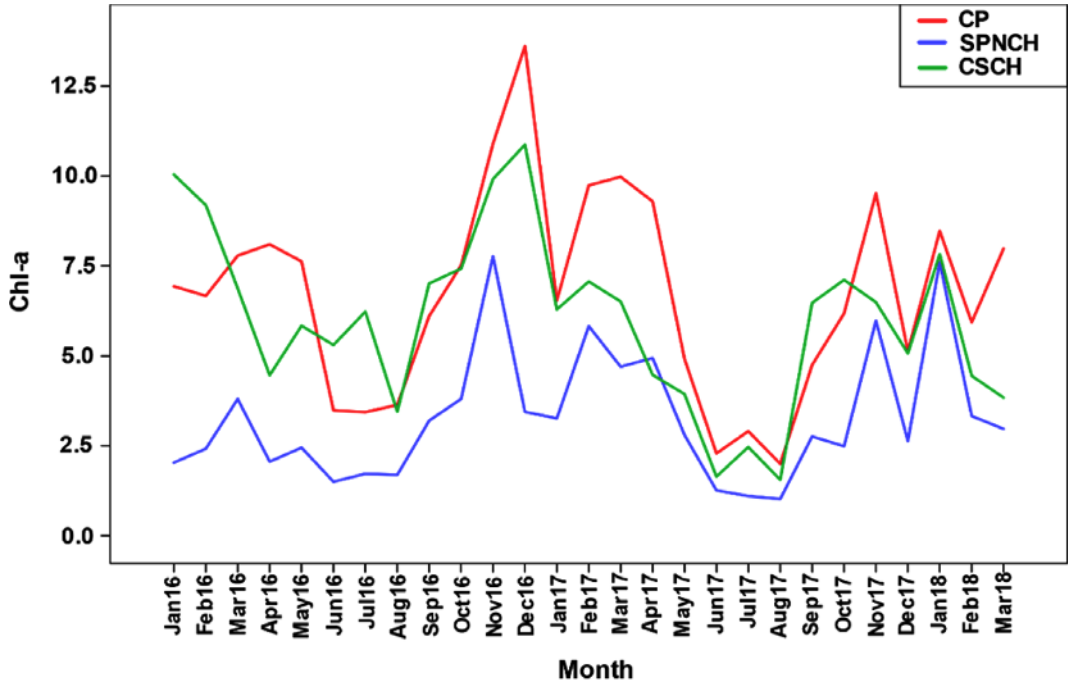

Fig. A1. Average surface chlorophyll-a concentration (Chl-a) (mgChl-a/m^3) in each population along the Humboldt Current between January 2016 and March 2018. CP = Central Peru, SPNCH = Southern Peru-Northern Chile, and CSCH = Central-Southern Chile

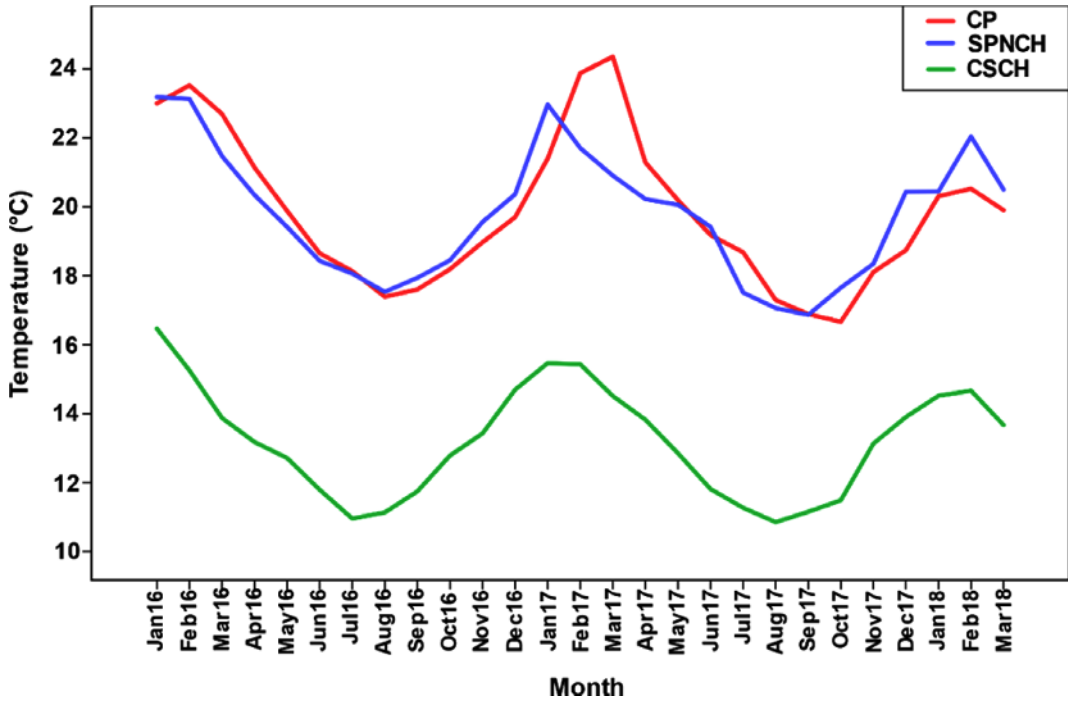

Fig. A2. Average sea surface temperature (SST) in each population along the Humboldt Current between January 2016 and March 2018. CP = Central Peru, SPNCH = Southern Peru-Northern Chile, and CSCH = Central-Southern